USCAP

ARTICLE

Enrichment of "Cribriform" morphologies (intraductal and cribriform adenocarcinoma) and genomic alterations in radiorecurrent prostate cancer

Rajal B. Shah[1]✉, Doreen N. Palsgrove[1], Neil B. Desai[2], Jeffrey Gagan[1], Amanda Mennie[2], Ganesh Raj[3] and Raquibul Hannan[2]

Locally relapsed prostate cancer (PCa) after radiation therapy (RT) is associated with substantial morbidity and mortality. Morphological and molecular consequences that may contribute to RT resistance and local recurrence remain poorly understood. Locally recurrent PCa tissue from 53 patients with clinically localized PCa who failed with primary RT and subsequently underwent salvage radical prostatectomy (RP) was analyzed for tumor focality, clinicopathological, molecular, and genomic characteristics. Targeted next-generation sequencing with full exon coverage of 1,425 cancer-related genes was performed on 10 representative radiorecurrent PCas exhibiting no RT effect with matched adjacent benign prostate tissue. At RP, 37 (70%) of PCas had no RT effect with the following characteristics: grade group (GG) ≥ 3 (70%), unifocal tumor (75%), extraprostatic disease (78%), lymph node metastasis (8%), and "cribriform" morphologies (84%) [cribriform PCa (78%) or intraductal carcinoma (IDC-P) (61%)] at a median percentage of approximately 80% of tumor volume. In the setting of multifocal tumors (25%) at RP, the cribriform morphologies were restricted to index tumors. Of 32 patients with available pre-RT biopsy information, 16 had GG1 PCa, none had cribriform morphologies at baseline but 81% demonstrated cribriform morphologies at RP. Notable alterations detected in the sequenced tumors included: defects in DNA damage response and repair (DDR) genes (70%) (*TP53*, *BRCA2*, *PALB2*, *ATR*, *POLQ*), *PTEN* loss (50%), loss of 8p (80%), and gain of *MYC* (70%). The median tumor mutational burden was 4.18 mutations/Mb with a range of 2.16 to 31.86. Our findings suggest that most radiorecurrent PCas are enriched in cribriform morphologies with potentially targetable genomic alterations. Understanding this phenotypic and genotypic diversity of radiorecurrent PCa is critically important to facilitate optimal patient management.

Modern Pathology (2022) 35:1468–1474; https://doi.org/10.1038/s41379-022-01093-9

INTRODUCTION

Recurrent prostate cancer (PCa) following radiation therapy (RT) in patients with clinically localized PCa has been shown to exhibit tropism for specific anatomical distributions with divergent prognoses[1]. In this setting, local recurrence in the prostate and seminal vesicle is a common first site of failure[1]. For patients with locally advanced recurrence, in particular, salvage with measures such as radical prostatectomy (RP) is not usually curative and is followed often by metastatic progression[2,3]. There are no established risk classification schemes guiding the management of locally radiorecurrent PCa, with outcomes generally associated with time to failure, PSA kinetics, initial clinical stage, and Gleason grade[4]. However, these risk classification factors do not account for the intratumoral spatial, morphological, and genomic heterogeneity that may provide treatment-resistant clones a survival advantage, thereby exhibiting a clinically aggressive course[4–6]. Understanding the morphological and molecular diversity that may contribute to the development of radioresistance and the risk of biochemical relapse and metastasis following definitive therapy is critically important.

Microenvironmental factors such as tumor hypoxia, adverse molecular indices such as genomic instability (percentage of genome alteration and copy number alterations), and adverse subpathologies such as intraductal carcinoma (IDC-P) and cribriform PCa have been linked to potential therapeutic resistance and disease recurrence[7,8]. Chua et al. proposed a novel concept of PCa defined by the constellation of unfavorable features characterized by genomic instability, increased hypoxia, and increased expression of long non-coding RNA *SCHLAP1*. This idea was termed '*nimbosus*', meaning a gathering of stormy clouds, and is associated with PCa harboring adverse subpathologies with poor prognosis following RP or image-guided radiotherapy[7].

Herein, we analyzed radiorecurrent cases of PCa in patients who underwent salvage RP and proceeded to demonstrate that tumors without treatment effect are enriched in both cribriform PCa and IDC-P, collectively referred to as cribriform morphologies, and exhibit genomic alterations that are often seen in advanced PCa. Our observations suggest that these recurrent tumors are likely driven by treatment-emergent clones that are either absent prior to the initiation of treatment, or present with an increased survival advantage relative to the pretreatment state. Understanding the

[1]Department of Pathology, University of Texas Southwestern Medical Center, Dallas, TX, USA. [2]Department of Radiation Oncology, University of Texas Southwestern Medical Center, Dallas, TX, USA. [3]Department of Urology, University of Texas Southwestern Medical Center, Dallas, TX, USA. ✉email: Rajal.Shah@UTSouthwestern.edu

Received: 19 February 2022 Revised: 23 April 2022 Accepted: 25 April 2022
Published online: 23 May 2022

phenotypic and genotypic diversity of recurrent PCa following RT is critically important to understanding radio-resistance and facilitating optimal patient management.

MATERIALS AND METHODS

Patient population

Using our institutional review-board approved database, consecutive patients with a diagnosis of clinically localized PCa over a span of 10 years between 2009 and 2019 were identified and included in this retrospective analysis. These patients had experienced clinical or biochemical recurrence after primary radiation as a definitive therapy, with or without additional androgen deprivation therapy (ADT), and had subsequently underwent salvage RP. Pre-RT prognostic factors including PSA, biopsy grade group, tumor volume (% core involvement), and family history of malignancy were collected when available. Initial RT was characterized by radiation modality, use of ADT (yes/no), time to subsequent failure (biochemical or clinical), and time to salvage RP.

Morphological categorization

Histopathological evaluation of entirely submitted whole-mount RP specimens served as the standard of reference. All tumors were systematically mapped and evaluated for tumor multifocality and inter-focal tumor heterogeneity by one author (RBS) as previously described[4]. For multifocal tumors, the largest tumor nodule was defined as the index tumor. Morphological features of PCa were divided into three groups: (1) tumor predominantly exhibiting RT effect (2) tumor without RT effect and (3) tumor exhibiting partial RT effect. Histological changes of PCas exhibiting RT treatment effect were determined based on cytoplasmic and nuclear characteristics, as demonstrated by Crook et al.[9]. Tumors without treatment effect were assigned a grade group (GG) based on the 2014 ISUP modified grading system[10], and each tumor focus was evaluated for the presence of adverse morphological features, specifically, invasive cribriform pattern 4 and IDC-P. The diagnosis of IDC-P and cribriform PCa was based on morphological features previously described[10,11]. Basal cell marker p63 was utilized to distinguish IDC-P from cribriform PCa when the presence of basal cells on hematoxylin and eosin slides was ambiguous[12]. Pathological staging of RP specimens was performed according to the 2016 AJCC staging criteria.

Molecular analysis

DNA and RNA sequencing were performed by the Once Upon a Time Human Genomics Center at UT Southwestern Medical Center. Tumor hematoxylin and eosin slides on 10 representative tumor samples without treatment effect and enriched in cribriform morphologies were marked for subsequent macrodissection, nucleic acid isolation, and molecular testing. Areas enriched with tumor growth were then scraped from adjacent 5µm thick formalin-fixed paraffin-embedded sections. Matched normal tissue was separately isolated and processed when available. Subsequent extraction and purification was performed using Qiagen Allprep kits (Qiagen, Germantown, MD). Libraries were prepared using KAPA Hyperplus kits (Roche Sequencing and Life Science Kapa Biosystems, Wilmington, MA) with genomic regions of interest captured by custom probes covering all exons of 1425 cancer-related genes. The libraries were sequenced using Sequencing by Synthesis paired-end cluster generation on the Illumina NextSeq. 550 platform (Illumina Inc., San Diego, CA), and the DNA sequence reads were aligned to reference genome GRCh38. Single nucleotide variants, insertions and deletions were called using Strelka2, MuTect2, Freebayes, and Platypus, with copy number alterations called using CNVKit. Aneuploidy was determined by the presence of chromosomal arm gains or losses, and tumor mutation burden (TMB) was calculated as the number of somatic mutations per mega base (Mb). Fusions were called using the STAR-Fusion algorithm with RNA-Seq reads (https://github.com/bcantarel/school). All fusions and variant calls were classified according to the Association for Molecular Pathology/American Society for Clinical Oncology/College of American Pathologists guidelines and they were manually inspected using Integrated Genomics Viewer (IGV; Broad Institute, MIT Harvard, Cambridge, MA).

RESULTS

Clinical parameters

The initial patient cohort was comprised of 53 patients who failed primary radiation as definitive therapy, based on biochemical failure or local recurrence, and subsequently underwent salvage RP. Of this initial cohort, patients exhibiting no morphological evidence of treatment effect at salvage RP were selected for further analysis.

Pathological features

Within the initial patient cohort, 30% had morphological evidence of either complete or partial RT treatment effect, while 70% exhibited no treatment effect. Only PCas exhibiting no treatment effect were further evaluated for grade group and adverse pathological features. Table 1 summarizes pathological and staging characteristics of the 37 patients who exhibited no treatment effect at RP. Briefly, 70% of patients exhibited GG ≥ 3, 78% had evidence of extraprostatic disease, 8% had lymph node metastasis, and 84% demonstrated cribriform morphologies (Fig. 1) including cribriform PCa in 78% of patients and IDC-P in 61%. Both morphologies were present in 49% of cases with the median percentage of cribriform PCa at 80% of tumor volume. A spectrum of morphologies was encountered in variable combinations in 6 patients with non-cribriform PCa: "poorly-formed glands" pattern 4 (6 cases), "fused glands" pattern 4 (4 cases), and "glomeruloid glands" pattern 4 (3 cases) (Supplemental Fig. 1). One specimen had a minor tertiary 5 component composed of tumor cords. One case exhibited prominent background atypical intraductal proliferation. Most patients demonstrated a unifocal tumor nodule at salvage RP. For patients with multifocal tumors, cribriform growth pattern, when present, was exclusively seen in the dominant/index tumor. Background benign prostate tissue demonstrated RT changes in the majority of specimens.

Pretreatment biopsy and clinical information

Pretreatment biopsy information in the group without treatment effect was available for 70% of patients. Of 16 patients with

Table 1. Pathological characteristics of 37 patients without morphological evidence of treatment effect at salvage radical prostatectomy.

Pathological characteristic	Number (%)
Median Index Tumor Size in mm	19.5 (range, 7–50)
Grade group	
1	0 (0)
2	11 (30)
3	10 (27)
4	9 (24)
5	7 (19)
Cribriform Morphology	
Cribriform prostate cancer (PCa)	28 (78)
Intraductal carcinoma	22 (61)
Cribriform PCa or Intraductal carcinoma	31 (84)
Cribriform PCa and Intraductal carcinoma	18 (49)
Median Percent Cribriform Morphology	80 (range, 2 to 100)
Tumor focality	
Focal	28 (75)
Multifocal	9 (25)
Pathologic stage	
pT2	8 (22)
pT3a	14 (38)
pT3b	13 (35)
pT4	2 (5)
Lymph node metastasis	3 (8)

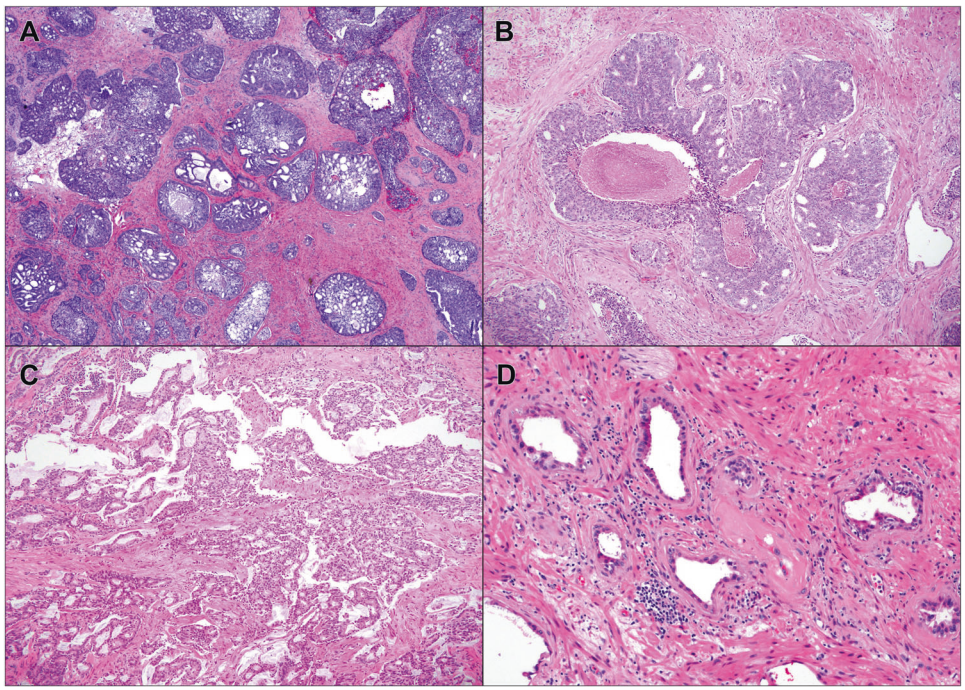

Fig. 1 A representative example of an index tumor in a salvage radical prostatectomy specimen exhibiting radiorecurrent prostate adenocarcinoma enriched in "cribriform" morphologies. A low power view of the index tumor exhibits proliferation of variably sized dense cribriform glands (**A**). Intraductal carcinoma of the prostate characterized by large expansile and branching glands with dense cribriform architecture and intraluminal comedonecrosis (**B**). Cribriform Gleason pattern 4 adenocarcinoma characterized by back-to-back confluent and infiltrative dense cribriform glands (**C**). The tumor lacks morphological evidence of radiation treatment effect but background benign prostate tissue exhibits morphological evidence of radiation therapy (**D**).

pretreatment biopsy GG1 without IDC-P, 81% exhibited cribriform morphologies at RP. Upgrading of GG from pre-RT biopsy at the time of salvage RP was observed in 77% of post-RT recurrent tumors. Table 2 summarizes clinical, pretreatment biopsy characteristics, treatment information, time to salvage treatment, and time to failure of these 37 patients. Table 3 summarizes clinical, biopsy characteristics, treatment information, salvage RP findings, time to salvage treatment, and time to failure specifically for a subgroup of 16 patients with baseline biopsy GG1 without cribriform morphologies. Of note, thirteen patients received androgen deprivation treatment in addition to radiation treatment. The frequency of cribriform morphologies was 75% in patients treated with radiation treatment alone versus 92% in patients treated with radiation treatment with additional androgen deprivation therapy (ADT).

Family history of malignancy in first-degree relatives was reported in eight of ten cases, and the median time to RT failure was 6 months, ranging from one to 17 months.

Genomic alterations

Supplementary Table 1 and Fig. 2 summarize genomic alterations observed in 10 radiorecurrent PCa samples enriched in cribriform morphologies. One case failed RNA sequencing. Notable genetic alterations included: *ETS* fusions (5 of 9 cases); mutations in various DNA damage response and repair (DDR) genes [7 of 10 cases – *TP53* (3 cases), *BRCA2* (1 case), *PALB2* (1 case), *POLQ* (1 case), *ATR* (1 case), *FANCB* (1 case), *BARD1* (1 case)]; activating mutations in *PIK3CA* (1 case) and *SPOP* (1 case); and alterations involving *PTEN* (2 cases), *KMT2D* (3 cases), *RNF43* (1 case), *FOXA1* (1 case), *STAT3* (1 case), *PPP2R2A* (1 case), and *CTNNB1* (1 case). Notable chromosomal alterations included: loss of 8p involving *NKX3-1* and *PPP2R2A* (9 cases); loss of 13q involving *FOXO1, BRCA2*, and/or *RB1* (5 cases); loss of 17q (6 cases); loss of 16q (4 cases); 17p loss or copy neutral loss of heterozygosity (LOH) involving *TP53* (5 cases); loss of 10q involving *PTEN* (3 cases); loss of 18q (3 cases); gain of 8q involving *MYC* (7 cases); and whole chromosome gains of chromosome 7 (3 cases). Notably, a rare *PRIM2-BRAF* fusion was detected in case 9. Furthermore, a single Tier 1 variant of strong clinical significance, *PTEN* p.Gln245*, was identified while all other variants were considered Tier 2 or Tier 3.

TMB ranged from 2.16 to 31.86 mutations/Mb, with a mean of 6.77 mutations/Mb and a median of 4.18 mutations/Mb. Of note, one tumor demonstrated hypermutation with 119 somatic alterations. All tumors were considered microsatellite stable, and aneuploidy, defined as chromosomal arm gains or losses, was detected in all specimens.

Matched normal tissue was evaluated for abnormalities in *BRCA1/2, BARD1, BRIP1, PALB2, CHEK1/2, RAD51, RAD51B/C/D, ATM, ATR, MSH2/3/6, MLH1/3, PMS2, EPCAM, HOXB13, NBN, GEN1, TP53, FANCA/L* genes. Variants of uncertain significance were detected in *BARD1* (p.Val507Met; p.Leu359_Pro365del; p.Arg731Gly), *RAD51B* (p.Val207Leu), *EPCAM* (p.Ile193Val), *FANCA* (p.Leu1143Val), *MSH3* (p.Arg411His), *ATM* (p.Asn1005Ser), *MSH6* (p.Gly571Asp; p.Pro1073-Ser), *NBN* (p.Tyr749Phe), *BRCA1* (c.5216-3T > C; p.Val1825Asp), *BRCA2* (p.Asn56Thr), *BRIP1* (p.Arg173Cys), and *HOXB13* (p.Ter285fs).

DISCUSSION

To our knowledge, this is the first study that addresses phenotypic and genotypic characteristics of radiorecurrent, locally advanced PCas. Salvage prostatectomies are a rare phenomenon owing to a low rate of detected PCa local failures after definitive radiation and worries of surgical difficulties and complications in a previously radiated field where scar tissue is expected to form. There were a limited number of retrospective clinical series and one small prospective multicenter trial reporting on salvage prostatectomy spanning the last three decades[13–15].

In this study, we show that radiorecurrent, locally advanced PCas exhibit over representation of cribriform morphologies. There is now robust evidence that both IDC-P and cribriform

Table 2. Pre-treatment clinical information, treatment modality, and follow-up information for 37 patients with morphological evidence of no treatment effect in prostate cancer at salvage radical prostatectomy.

Clinical, treatment-modality and follow up information	Number (%)
Median age in years	69 (range, 54–78)
Median PSA (ng/ml) at diagnosis	5.15 (range, 3.1–12)
Biopsy grade group	
1	16 (43)
2	9 (24)
3	2 (5)
4	1 (3)
5	1 (3)
NA	8 (21)
Median percent core involvement	33 (range, 5–90)
Type of radiation treatment	
IMRT	12
Brachytherapy	9
XRT	3
Brachytherapy + XRT	2
Proton therapy	1
HDR	1
NA	9
Androgen deprivation therapy	
Yes	13
No	19
Median time in months from dx to recurrence	6 (range, 1–17)
Median time in months from dx to salvage RP	7 (range, 1–17)

NA not available, *RP* radical prostatectomy, *IMRT* intensive modulated radiation therapy, *XRT* radiation therapy, *HDR* high dose rate brachytherapy, *dx* diagnosis.

Table 3. Clinical, biopsy, treatment modality and salvage RP characteristics for subgroup of 16 patients with baseline biopsy grade group 1 prostate cancer without cribriform morphologies.

Clinical, biopsy, treatment modality, and salvage RP characteristic	Number (%)
Median Age in years	69 (range, 54–75)
Median PSA (ng/ml) at diagnosis	5 (range, 3.4–10.8)
Mean number of biopsy cores sampled	11 (range, 6–14)
Median percent core tumor involvement	25 (range, 5–46)
Type of radiation treatment	
IMRT	3
Brachytherapy	8
XRT	2
Brachytherapy + XRT	1
NA	2
Androgen deprivation therapy	
Yes	5
No	9
Median time in months from dx to recurrence	6 (range, 2 to 17)
Median time in months from dx to salvage RP	7 (range, 2 to 17)
RP grade group	
1	0 (0)
2	5 (31)
3	2 (12)
4	3 (19)
5	6 (38)
RP morphology	
Cribriform PCa	12 (75)
IDC-P	9 (56)
Cribriform PCa or IDC-P	14 (87)
Both	9 (56)

NA not available, *RP* radical prostatectomy, *IMRT* intensive modulated radiation therapy, *XRT* radiation therapy, *PCa* prostate cancer, *IDC-P* intraductal carcinoma.

pattern PCa are independent adverse prognostic morphological parameters in a variety of treatment settings[16–21]. In needle biopsy settings, these parameters are associated with a variety of adverse outcomes, including lymph node metastasis and worsened disease-specific survival. Many centers regard the presence of such histologic patterns in needle biopsy as an exclusion criterion for active surveillance. Tom et al. analyzed the impact of cribriform pattern and intraductal carcinoma on Gleason 7 PCa treated with external beam radiotherapy and demonstrated that cribriform patterns with IDC-P were associated with adverse outcomes[22]. Van der Kwast et al. demonstrated that IDC-P in diagnostic samples of patients with intermediate or high-risk prostate cancer is an independent prognosticator of early biochemical relapse and metastatic failure rate after radiotherapy[23]. Due to their shared association with adverse clinical outcomes, molecular characteristics, and as the majority of IDC-P exhibit cribriform architecture and represent a retrograde spread of high-grade and high volume PCa, some authors have grouped both morphologies into a single prognostic group of PCa with cribriform morphologies[17,19,20,24]. Clinical and pathological characteristics of cases in this cohort are concordant with the known adverse association of PCa demonstrating cribriform morphologies. The majority of recurrent PCas following RT in this study had locally advanced disease. The extraprostatic disease was seen in 78% of cases with 35% presenting with seminal vesicle involvement, and 8% with invasion of adjacent organs. In addition, lymph node metastasis was present in 8% of cases. These results suggest that for patients with radiorecurrent PCa showing cribriform morphologies, local control alone in form of salvage RP may not be an adequate strategy, as the risk of rapid failure or metastasis is significantly higher. This is corroborated by the poor disease control seen following salvage RP for a relatively unselected population in CALGB 9687, where approximately 50% and 75% of men failed biochemically by two and 10 years after salvage RP, respectively[14]. In contrast, RTOG 0526 achieved 54% freedom from biochemical failure at 10 years after brachytherapy (radioactive seed implant) salvage in a more selected population of men[25]. Given such heterogeneous outcomes and the morbidity of salvage therapy, it is of great need to identify correlates to mechanisms of metastagenesis and therapeutic resistance for these men to direct treatment focus and type.

Indeed, our data suggests that "enrichment" of cribriform morphologies in radiorecurrent PCa may occur potentially through three mechanisms: from treatment-emergent clones in response to selective pressure, RT-induced changes or over-representation in patients selected for radiotherapy. The frequency of this growth pattern was unusually high in

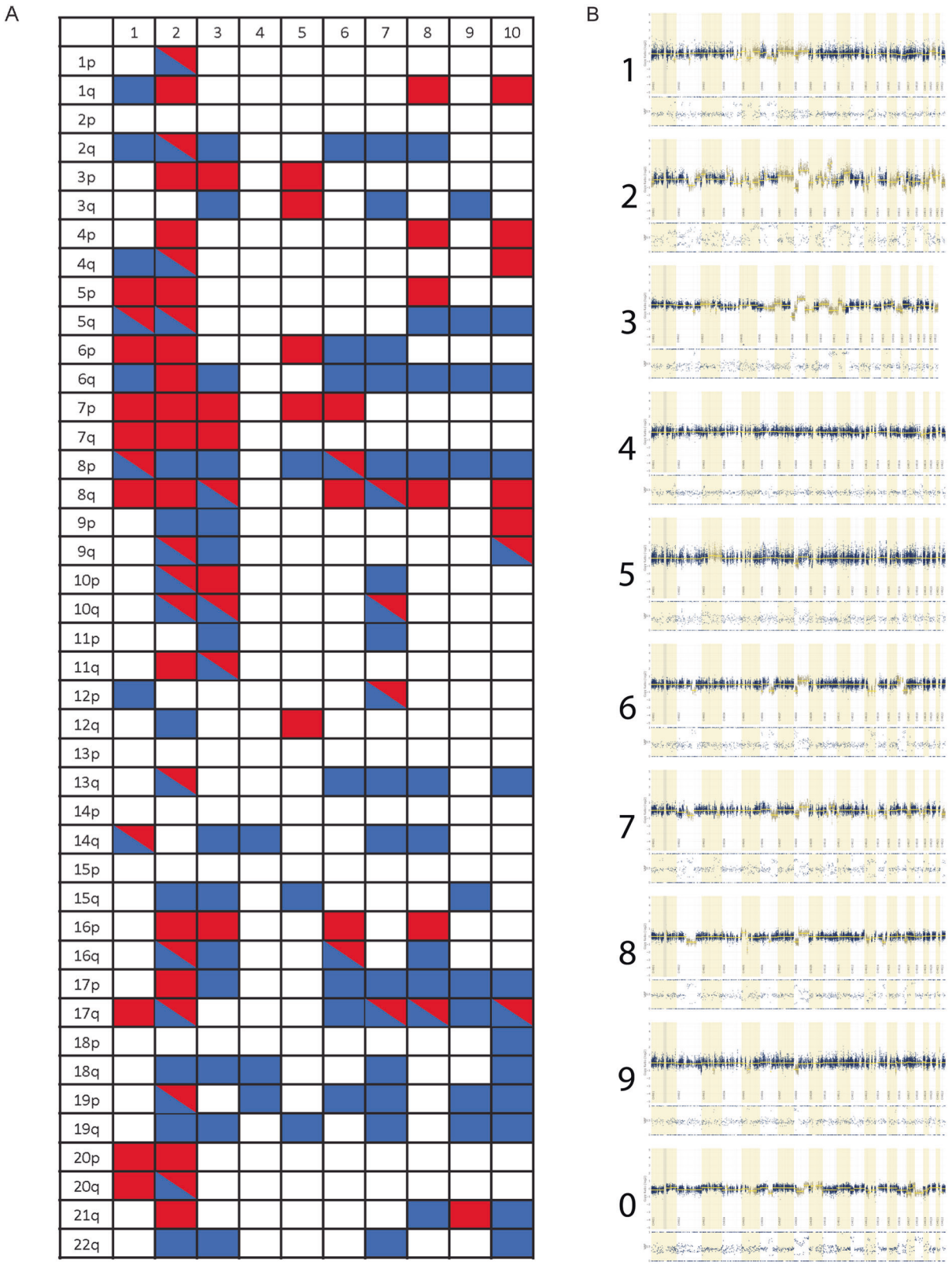

Fig. 2 Copy number alterations observed in radiorecurrent prostate carcinoma samples enriched in "cribriform" morphologies. The presence of focal, segmental, or whole chromosomal arm gains (red) and losses (blue) by chromosome are shown for each case (**A**) along with segment log2 ratios and single-nucleotide variant allele frequencies (**B**).

posttreatment PCa samples in comparison to what has been reported in clinically localized treatment naïve PCa. In the Cancer Genome Atlas Project and the Canadian Prostate Cancer Genome Network RP datasets, PCa with cribriform morphologies was present in 31% and 38% of tumors, respectively[26]. In comparison, with this cohort, cribriform morphologies were observed in 89% of cases. In addition, of 16 patients with pretreatment biopsy GG1, 81% exhibited cribriform morphologies only at RP, suggesting that these subpathologies were not present or were not the dominant clone in a significant number of pretreatment samples. Finally, primary treatment-naïve localized PCa are typically a multifocal group of diseases with significant inter-focal morphological and molecular heterogeneity[6]. In comparison, radiorecurrent PCas were predominantly unifocal disease. For patients who demonstrated multifocal tumors, only index or dominant tumors contained adverse subpathologies. Smaller tumors either lacked these adverse morphologies or exhibited the RT effect. Collectively, these data suggest that development of cribriform morphologies appears a hallmark of treatment emergent aggressive disease, whether developing from occult sub-clonal initial disease or a new clone following radiation failure. Indeed, clinical relevance of such index lesions to RT resistance was confirmed further by the demonstration of significantly improved disease control using MRI-guided lesion RT boosts of initial index lesions in the recently published phase III FLAME trial[27].

Molecular features of radiorecurrent PCas enriched in cribriform morphologies analyzed from this study are comparable to treatment-naïve PCas enriched in cribriform morphologies[12,28]. Using the Cancer Genome Atlas cohort, Elfandy et al. studied genetic and epigenetic determinants of aggressiveness in cribriform carcinoma[28]. Distinct molecular features included increased somatic copy number variations, specifically deletions at 6q, 8p, and 10q, which encompassed *PTEN* and *MAP3K7* losses and gains at 3q; increased *SPOP* mutations and *ATM* mutations; and enhancements for mTORC1 and MYC pathways by gene expression. Validation in clinical cohorts and murine models confirmed the association with *SPOP* mutations and *PTEN* losses. When compared with metastatic prostate cancer, invasive cribriform cancer clustered more closely to metastatic PCa than non-cribriform Gleason pattern 4, suggesting that invasive cribriform cancer has a distinct molecular phenotype that resembles metastatic PCa and is associated with progression to lethal disease[28].

Notable variants of clinical significance present in these samples that have shown an association with progression to advanced and metastatic PCa included defects in one or more DDR genes (70% of samples), specifically *TP53*, *BRCA1/2*, *PALB2*, *ATR*, *POLQ*, *FANCB*, and *BARD1* mutations, and *PTEN* loss (50%). In one study, 14% of patients with lethal PCa were found to have alterations in *BRCA2*[29]. The whole-exome sequencing results of the initial 150 metastatic castration-resistant PCa metastases from SU2C Prostate International Dream Team demonstrated that 19% had aberrations in DDR genes including *BRCA1*, *BRCA2*, and *ATM*[30,31]. Our samples also demonstrated less frequently encountered variants of clinical significance in *KMT2D*, *KDM6A*, *PIK3CA*, *STAT3*, *PPPR2A, SPOP*, and *FOXA1*. *KDM6A* is associated with the progression of the lethal castration-resistant disease[29] while *PIK3CA* mutations with concurrent *PTEN* loss have been shown to cooperatively accelerate and facilitate castration-resistant disease in vivo[32]. *PTEN* loss is also independently associated with an increased risk of lethal progression, particularly in patients without *ERG* fusions[33]. Interestingly, a rare *PRIM2-BRAF* fusion was noted in one case. This rearrangement, although rare, tends to occur in advanced metastatic PCa[29]. Furthermore, many of these alterations provide targets for specific therapeutic interventions. Defects in homologous recombination DNA repair pathway genes, specifically deleterious mutations in *BRCA1/2*, *BARD1*, and *PALB2* amongst others, have shown sensitivity to poly-ADP ribose polymerase (PARP) inhibitors with an overall survival benefit in men with metastatic castration-resistant PCa[34,35]. Similarly, *KMT2C/D* mutations may confer sensitivity to PARP inhibitors such as olaparib (39), while biallelic loss of *MAP3K1* is associated with response to MEK inhibitors[36]. Furthermore, *TP53* mutations may predict resistance to a new generation of AR-targeted enzalutamide or abiraterone therapy[37].

Despite these important observations, this study has limitations. The cohort studied was retrospectively identified and thus, imaging, treatment endpoints, and morphological and sequencing of tissue samples were not prospectively defined, collected, or performed. There is also lack of a well-defined control group for comparisons of our novel findings and selection is subject to interobserver variation[11]. In addition, we did not have pretreatment biopsy archival tissue material available as a paired sample to analyze pre- and post-treatment differences that may exist in relation to morphology, tissue hypoxia, and genomic landscape. Finally, only the worst players with no RT effect were analyzed and only a subset of samples that were deemed representative of radiorecurrent PCa could be sequenced for molecular analysis. In light of these limitations, our observations provide an important framework for future prospective studies.

In conclusion, we show that post RT failure PCas are enriched in cribriform morphologies and specific genomic alterations. Based on the unusually high frequency of these aggressive subpathologies in posttreatment samples, as well as the unifocal nature of tumors at RP, we speculate that they represent resistant tumor clones that emerge through selective pressure and/or RT-induced changes. Importantly, understanding of phenotypic and genotypic characteristics of recurrent PCa following RT provides important insight into optimal patient management, such as providing the basis for early detection of DDR-altered disease, and thus the potential benefit of PARP inhibitors.

DATA AVAILABILITY

All data generated or analyzed during this study are included in this published article (and its supplementary information files)

REFERENCES

1. Zumsteg ZS, Spratt DE, Romesser PB, Pei X, Zhang Z, Kollmeier M, et al. Anatomical patterns of recurrence following biochemical relapse in the dose escalation era of external beam radiotherapy for prostate cancer. J Urol 194, 1624-1630 (2015).
2. Mohler JL, Antonarakis ES. NCCN Guidelines Updates: Management of Prostate Cancer. J Natl Compr Canc Netw 17, 583-586 (2019).
3. Mohler JL, Antonarakis ES, Armstrong AJ, D'Amico AV, Davis BJ, Dorff T, et al. Prostate Cancer, Version 2.2019, NCCN Clinical Practice Guidelines in Oncology. J Natl Compr Canc Netw 17, 479-505 (2019).
4. Zumsteg ZS, Spratt DE, Pei I, Zhang Z, Yamada Y, Kollmeier M, et al. A new risk classification system for therapeutic decision making with intermediate-risk prostate cancer patients undergoing dose-escalated external-beam radiation therapy. Eur Urol 64, 895-902 (2013).
5. Cooper CS, Eeles R, Wedge DC, Van Loo P, Gundem G, Alexandrov LB, et al. Analysis of the genetic phylogeny of multifocal prostate cancer identifies multiple independent clonal expansions in neoplastic and morphologically normal prostate tissue. Nat Genet 47, 367-372 (2015).
6. Mehra R, Han B, Tomlins SA, Wang L, Menon A, Wasco MJ, et al. Heterogeneity of TMPRSS2 gene rearrangements in multifocal prostate adenocarcinoma: molecular evidence for an independent group of diseases. Cancer Res 67, 7991-7995 (2007).
7. Chua MLK, Lo W, Pintilie M, Murgic J, Lalonde E, Bhandari V, et al. A Prostate Cancer "Nimbosus": Genomic Instability and SChLAP1 Dysregulation Underpin Aggression of Intraductal and Cribriform Subpathologies. Eur Urol 72, 665-674 (2017).
8. Hieronymus H, Schultz N, Gopalan A, Carver BS, Chang MT, Xiao Y, et al. Copy number alteration burden predicts prostate cancer relapse. Proc Natl Acad Sci U S A 111, 11139-11144 (2014).
9. Crook JM, Malone S, Perry G, Eapen L, Owen J, Robertson S, et al. Twenty-four-month postradiation prostate biopsies are strongly predictive of 7-year disease-

free survival: results from a Canadian randomized trial. Cancer 115, 673-679 (2009).
10. Epstein JI, Amin MB, Fine SW, Algaba F, Aron M, Baydar DE, et al. The 2019 Genitourinary Pathology Society (GUPS) White Paper on Contemporary Grading of Prostate Cancer. Arch Pathol Lab Med (2020).
11. Shah RB, Cai Q, Aron M, Berney DM, Cheville JC, Deng FM, et al. Diagnosis of "cribriform" prostatic adenocarcinoma: an interobserver reproducibility study among urologic pathologists with recommendations. Am J Cancer Res 11, 3990-4001 (2021).
12. Shah RB, Shore KT, Yoon J, Mendrinos S, McKenney JK, Tian W. PTEN loss in prostatic adenocarcinoma correlates with specific adverse histologic features (intraductal carcinoma, cribriform Gleason pattern 4 and stromogenic carcinoma). Prostate 79, 1267-1273 (2019).
13. Devos G, Joniau S. Salvage prostatectomy for recurrent disease. Nat Rev Urol 16, 150-151 (2019).
14. Mohler JL, Halabi S, Ryan ST, Al-Daghmin A, Sokoloff MH, Steinberg GD, et al. Management of recurrent prostate cancer after radiotherapy: long-term results from CALGB 9687 (Alliance), a prospective multi-institutional salvage prostatectomy series. Prostate Cancer Prostatic Dis 22, 309-316 (2019).
15. Stephenson AJ, Eastham JA. Role of salvage radical prostatectomy for recurrent prostate cancer after radiation therapy. J Clin Oncol 23, 8198-8203 (2005).
16. Chua MLK, van der Kwast TH, Bristow RG. Intraductal Carcinoma of the Prostate: Anonymous to Ominous. Eur Urol 72, 496-498 (2017).
17. Iczkowski KA, Paner GP, Van der Kwast T. The New Realization About Cribriform Prostate Cancer. Adv Anat Pathol 25, 31-37 (2018).
18. Kato M, Tsuzuki T, Kimura K, Hirakawa A, Kinoshita F, Sassa N, et al. The presence of intraductal carcinoma of the prostate in needle biopsy is a significant prognostic factor for prostate cancer patients with distant metastasis at initial presentation. Mod Pathol 29, 166-173 (2016).
19. Kweldam CF, Kummerlin IP, Nieboer D, Verhoef EI, Steyerberg EW, van der Kwast TH, et al. Disease-specific survival of patients with invasive cribriform and intraductal prostate cancer at diagnostic biopsy. Mod Pathol 29, 630-636 (2016).
20. Kweldam CF, Wildhagen MF, Steyerberg EW, Bangma CH, van der Kwast TH, van Leenders GJ. Cribriform growth is highly predictive for postoperative metastasis and disease-specific death in Gleason score 7 prostate cancer. Mod Pathol 28, 457-464 (2015).
21. McKenney JK, Wei W, Hawley S, Auman H, Newcomb LF, Boyer HD, et al. Histologic Grading of Prostatic Adenocarcinoma Can Be Further Optimized: Analysis of the Relative Prognostic Strength of Individual Architectural Patterns in 1275 Patients From the Canary Retrospective Cohort. Am J Surg Pathol 40, 1439-1456 (2016).
22. Tom MC, Nguyen JK, Luciano R, Mian OY, Stephans KL, Ciezki JP, et al. Impact of Cribriform Pattern and Intraductal Carcinoma on Gleason 7 Prostate Cancer Treated with External Beam Radiotherapy. J Urol 202, 710-716 (2019).
23. Van der Kwast T, Al Daoud N, Collette L, Sykes J, Thoms J, Milosevic M, et al. Biopsy diagnosis of intraductal carcinoma is prognostic in intermediate and high risk prostate cancer patients treated by radiotherapy. Eur J Cancer 48, 1318-1325 (2012).
24. van Leenders G, Verhoef EI, Hollemans E. Prostate cancer growth patterns beyond the Gleason score: entering a new era of comprehensive tumour grading. Histopathology 77, 850-861 (2020).
25. Crook JM, Zhang P, Pisansky TM, Trabulsi EJ, Amin MB, Bice W, et al. A prospective phase 2 trial of transperineal ultrasound-guided brachytherapy for locally recurrent prostate cancer after external beam radiation therapy (NRG Oncology/RTOG-0526). Int J Radiat Oncol Biol Phys 103, 335-343 (2019).
26. Bottcher R, Kweldam CF, Livingstone J, Lalonde E, Yamaguchi TN, Huang V, et al. Cribriform and intraductal prostate cancer are associated with increased genomic instability and distinct genomic alterations. BMC Cancer 18, 8 (2018).
27. Kerkmeijer LGW, Groen VH, Pos FJ, Haustermans K, Monninkhof EM, Smeenk RJ, et al. Focal Boost to the Intraprostatic Tumor in External Beam Radiotherapy for Patients With Localized Prostate Cancer: Results From the FLAME Randomized Phase III Trial. J Clin Oncol 39, 787-796 (2021).
28. Elfandy H, Armenia J, Pederzoli F, Pullman E, Pertega-Gomes N, Schultz N, et al. Genetic and Epigenetic Determinants of Aggressiveness in Cribriform Carcinoma of the Prostate. Mol Cancer Res 17, 446-456 (2019).
29. Grasso CS, Wu YM, Robinson DR, Cao X, Dhanasekaran SM, Khan AP, et al. The mutational landscape of lethal castration-resistant prostate cancer. Nature 487, 239-243 (2012).
30. Robinson D, Van Allen EM, Wu YM, Schultz N, Lonigro RJ, Mosquera JM, et al. Integrative clinical genomics of advanced prostate cancer. Cell 161, 1215-1228 (2015).
31. Roy R, Chun J, Powell SN. BRCA1 and BRCA2: different roles in a common pathway of genome protection. Nat Rev Cancer 12, 68-78 (2011).
32. Pearson HB, Li J, Meniel VS, Fennell CM, Waring P, Montgomery KG, et al. Identification of Pik3ca Mutation as a Genetic Driver of Prostate Cancer That Cooperates with Pten Loss to Accelerate Progression and Castration-Resistant Growth. Cancer Discov 8, 764-779 (2018).
33. Ahearn TU, Pettersson A, Ebot EM, Gerke T, Graff RE, Morais CL, et al. A Prospective Investigation of PTEN Loss and ERG Expression in Lethal Prostate Cancer. J Natl Cancer Inst 108, (2016).
34. Taylor RA, Fraser M, Livingstone J, Espiritu SM, Thorne H, Huang V, et al. Germline BRCA2 mutations drive prostate cancers with distinct evolutionary trajectories. Nat Commun 8, 13671 (2017).
35. VanderWeele DJ, Hussain M. PARP inhibitors in prostate cancer: practical guidance for busy clinicians. Clin Adv Hematol Oncol 18, 808-815 (2020).
36. Cancer Genome Atlas Research N. The molecular taxonomy of primary prostate cancer. Cell 163, 1011-1025 (2015).
37. De Laere B, Oeyen S, Mayrhofer M, Whitington T, van Dam PJ, Van Oyen P, et al. TP53 Outperforms other androgen receptor biomarkers to predict abiraterone or enzalutamide outcome in metastatic castration-resistant prostate cancer. Clin Cancer Res 25, 1766-1773 (2019).

ACKNOWLEDGEMENTS

We are grateful to Sepeadeh Radpour MA, MS for editing the manuscript. This work was partly supported by Dr. Charles T Ashworth Professorship in Pathology endowment fund.

AUTHOR CONTRIBUTIONS

RBS performed study concept and design; RBS, DNP, NBD, RH performed development of methodology and writing, review of the paper; RBS, DNP, JG, AM provided acquisition, analysis and interpretation of data, and statistical analysis; GR, RH provided technical support. All authors read and approved the final paper.

COMPETING INTERESTS

The authors declare no competing interests.

ETHICS APPROVAL AND CONSENT TO PARTICIPATE

The study was approved by the UT Southwestern Medical Center (UTSW) Institutional Review Board and according to the Health Insurance Portability and Accountability Act (HIPAA) guidelines. Informed consent was waived due to the retrospective nature of the study.

ADDITIONAL INFORMATION

Supplementary information The online version contains supplementary material available at https://doi.org/10.1038/s41379-022-01093-9.

Correspondence and requests for materials should be addressed to Rajal B. Shah.